

Syntheses, Structures and Magnetic Properties of Layered Metal(II) Mandelates

Adel Beghidja,^[a,b] Sylvain Hallynck,^[a] Richard Welter,^{*,[b]} and Pierre Rabu^{*,[a]}

Keywords: Carboxylate ligands / Layered compounds / Magnetic properties / Transition metals / X-ray powder diffraction

A series of Mn^{II}, Fe^{II}, Co^{II}, Ni^{II} and Cu^{II} layered mandelates has been synthesised in the form of crystalline powders by a hydrothermal route. The five compounds are isostructural with the copper analogue, also obtained in a single crystal form, except that the latter shows a strong Jahn–Teller distortion of the coordination spheres around the Cu^{II} centres. The complexes crystallise in the monoclinic centrosymmetric space group $P2_1/a$ and their structures consist of layers of six-coordinate metal(II) ions interconnected through carboxylate

bridges in a diamond-like network. The magnetic data indicate very small antiferromagnetic in-plane couplings for **1**, **2**, **3** and **5**, with $J/k_B = -0.122$ K for **1**. The Ni^{II} compound **4** exhibits ferromagnetic coupling within the layers ($J/k_B = +1.213$ K) and ferromagnetic 3D ordering can be observed at $T_C = 2.7$ K.

(© Wiley-VCH Verlag GmbH & Co. KGaA, 69451 Weinheim, Germany, 2005)

Introduction

Correlations between the magnetic properties of molecule-based solids and their structures together with the nature of the chemical bond are useful in the design of new magnetic materials.^[1,2] In this respect, low dimensional systems in which the magnetic centres interact within chains (1D) or planes (2D) are of particular interest since their physics may be approximated and analysed to a high degree. This has been possible thanks to the development of a substantial amount of experimental and theoretical work in the area over several decades^[3–6] and to the efforts of synthetic chemists in providing model compounds, particularly through the molecular approach, i.e. by using molecular building blocks for the design of new interconnected networks,^[7,8] involving several kinds of metallic ions or radicals, which exhibit predictable magnetic properties.^[9–11] Focusing on 2D systems, as found in layered transition metal compounds, it has been shown that the occurrence of 3D magnetic ordering is mainly driven by the divergence of the correlation length within the layers which depends on the in-plane magnetic exchange coupling and on the topology of the magnetic centres.^[4,6,12,13] Recent results on organic-inorganic layered magnets have shown that it is possible to tune the coupling between spin layers by using suitable organic ligands separating or connecting transition

metal based layers.^[14] Striking results have been obtained in the field of low dimensional magnetic materials exhibiting unusual behaviour, by carrying out solvothermal reactions.^[15–19] In particular, recent reports have been concerned with the use of carboxylate moieties as bridging ligands between paramagnetic transition metal ions with the versatility of the carboxylate coordination group leading to magnetic networks with various topologies.^[20–23]

Our recent investigation of Co^{II} alkanates $[\text{Co}(\text{O}_2\text{C}(\text{CH}_2)_n\text{CH}_3)_2(\text{H}_2\text{O})_2]_n$ has shown that for long alkane chains, layered structures are obtained when the magnetic layers consist of chains of Co^{II} ions interconnected through carboxylate bridges in a *syn-anti* configuration. This leads to weak antiferromagnetic coupling.^[24] On the other hand, results on transition metal phenoxyalkanoate hydrates $[\text{M}(\text{O}_2\text{C}(\text{CH}_2)\text{OC}_6\text{H}_4\text{R})_2(\text{H}_2\text{O})_2]_n$ (M = Mn, Co; R = H, Cl, F, ...), the structures of which consist of stacked metal(II) carboxylate layers separated by an organic sub-network of phenyl rings, provided suitable examples of square planar arrays of magnetic centres.^[25,26] The diaquabis(phenoxyacetato)manganese(II) derivative exhibits typical behaviour for an antiferromagnetic 2D square-planar $S = 5/2$ system down to $T_C = 1.633$ K where a 3D ordered spin state leads to weak ferromagnetism. Magnetic data for the Co^{II} analogue suggest the presence of ferromagnetic interactions.^[27]

As a continuation of our investigations of layered systems, the present work is concerned with the synthesis, through a hydrothermal route, of a series of layered transition metal (M) carboxylates obtained using the chiral mandelate ion $\text{C}_6\text{H}_5\text{CH}(\text{OH})\text{CO}_2^-$ (M = Mn, Fe, Co, Ni, Cu) and an analysis of their crystal structures and magnetic

^[a] Institut de Physique et Chimie des Matériaux de Strasbourg, UMR 7504 du CNRS, 23 rue du Loess, 67034 Strasbourg, France
Fax: (internat.) + 33-3-88107247
E-mail: pierre.rabu@ipcms.u-strasbg.fr

^[b] Laboratoire DECMET, ILB, Université Louis Pasteur, 4 rue Blaise Pascal, 67000 Strasbourg, France

behaviour. Some molecular complexes of transition metals (Cu, Co, V) have been reported in the literature in which the mandelate anion acts as a co-ligand with lactic acid derivatives such as phenanthroline or bipyridine, resulting in peculiar coordination geometries.^[28–31] Noble metal complexes were also prepared.^[32] It is worth noticing, however, that very few results have been reported in the literature on compounds involving only the mandelate ion and most of these studies have concerned the solubility, vibrational spectroscopic properties and optical activities of the isolated metal complexes.^[33] Only one very recent work reports the crystal structure and magnetic susceptibility measurements of a Co^{II} derivative.^[34]

Results and Discussion

Synthesis and Structural Analysis

A series of five transition metal mandelates has been synthesised through a hydrothermal method by treating metal chlorides with mandelic acid and NaOH in water (see Experimental Section). The complexes of manganese (**1**), iron (**2**), cobalt (**3**) and nickel (**4**) were obtained as crystalline powders consisting of very thin platelets. The Fe^{II} solid **2** contains a small amount of a magnetic impurity, namely iron oxide, which was revealed by the magnetic measurements. The copper(II) analogue **5** crystallises from the mother solution (resulting from hydrothermal treatment) as thick single crystals suitable for X-ray analysis. It is worth noticing also that reactions under standard conditions at room temperature led, for the five metal ions, to the same products but only as fine and less crystalline powders. This highlights the importance of an interest in the hydrothermal method. The structure of **5** has been solved by a single-crystal X-ray diffraction analysis (see crystallographic section) and is similar to that reported in the literature for the Co^{II} analogue^[34] except that an accurate Fourier analysis ascertained the presence of the hydrogen of the α -hydroxide coordinated to the copper(II) centres, whereas this was not considered for the cobalt species. The compound can be described as a (diaqua)copper(II)- μ -mandelate polymer, the asymmetric unit of which is displayed in Figure 1. Each Cu^{II} atom is coordinated to six oxygen atoms forming elongated octahedra. In the equatorial plane, they are surrounded by two mandelate ligands each chelating the metal through one oxygen atom of the carboxylate group [Cu–O1 1.924(2) Å] and the α -OH [Cu–O2 1.987(2) Å]. Two other mandelate groups complete the octahedral site with monodentate oxygen atoms from their carboxylate functions in apical positions [Cu–O3#1 2.418(2) Å] resulting in a distorted environment (Figure 1) similar to the Co^{II} case but with strong additional distortion of the octahedral sites around metal ions due to the Jahn–Teller effect (see Table 1).

Within the a, b planes, the copper atoms are connected to four neighbours by carboxylato bridges in a *syn-anti* conformation (Figure 1), thus forming square-planar magnetic arrays separated by a double layer of mandelate anions

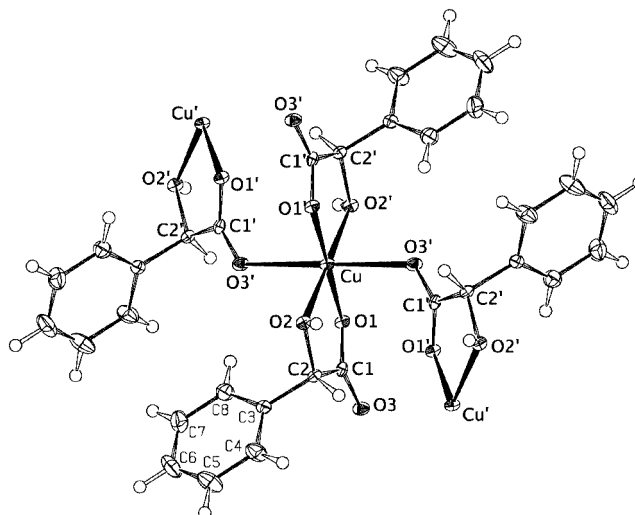


Figure 1. ORTEP plot of the structure of **5** showing coordination of the Cu^{II} atoms by the mandelate ligands and interconnection through carboxylato bridges

Table 1. Bond lengths [Å] and angles [°] in the copper dimandelate compound

Atoms	Distances	Atoms	Angles
Cu–O1	1.924(2)	O1–Cu–O2	83.41(10)
Cu–O2	1.987(2)	O1–Cu–O2#2	96.59(10)
Cu–O3#1	2.418(2)	O1–Cu–O3#1	95.18(9)
O1–C1	1.299(4)	O1#2–Cu–O3#1	84.82(9)
C1–C2	1.530(5)	O2–Cu–O3#1	95.18(9)
O2–C2	1.466(3)	O2#2–Cu–O3#1	89.63(9)
C2–C3	1.506(4)	C1–O1–Cu	115.72(19)
		C2–O2–Cu	113.32(18)
O1#3–O2#2 (intermolecular)	2.752(4)	O3–C1–O1	123.5(3)
		O3–C1–C2	119.1(3)

#1: $-x + 1/2, y + 1/2, -z + 1$; #2: $-x + 1, -y, -z + 1$; #3: $-x + 1, -y + 1, -z + 1$

(Figure 2). The Cu–Cu distances across the carboxylato bridges are 5.325(5) Å which correspond to the exchange pathways schematised in Figure 3. Moreover, intermolecular hydrogen bonds can be identified [O1#3–O2#2 2.752(4) Å, O1–H1–O2 171°], the CuO₆ octahedra thus being connected by two O1–O2 hydrogen bonds along the b axis. All the mandelates are positioned quasi-perpendicular to the copper layers which are 15.12(1) Å apart. In addition, a detailed examination of the structural stacking prompts a consideration of the existence of σ – π interactions between the phenyl rings related symmetrically by the crystallographic a mirror plane. (Figure 2).^[35] These cycles form an angle of 87° and the centroid–centroid distance is 5.21 Å. The shortest distances for σ – π interactions are: C4–C8 3.70 Å, C4–C7 3.74 Å, C5–C7 3.93 Å and C5–C6 4.19 Å.

It is apparent that the structure is centrosymmetric. Accordingly, the present compounds exhibit no circular dichroism and involve both (*R*) and (*S*) enantiomers of the mandelate ligand although the pure (*R*) enantiomer was used as a starting ligand. This was also observed in the

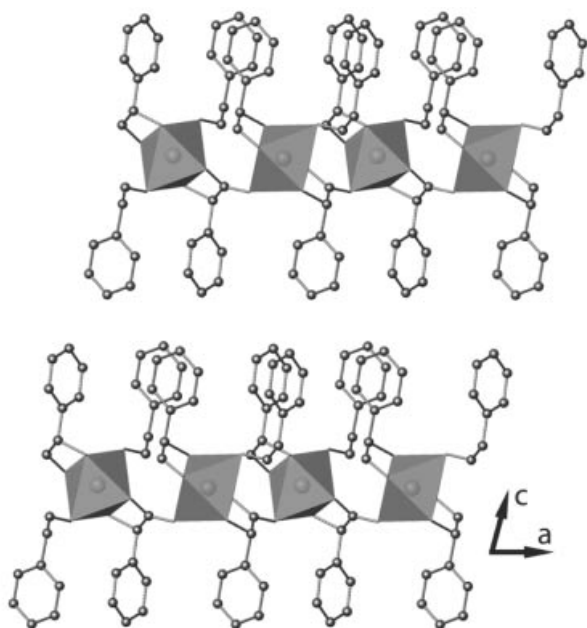


Figure 2. Partial view along the b axis of the layered structure of **5**

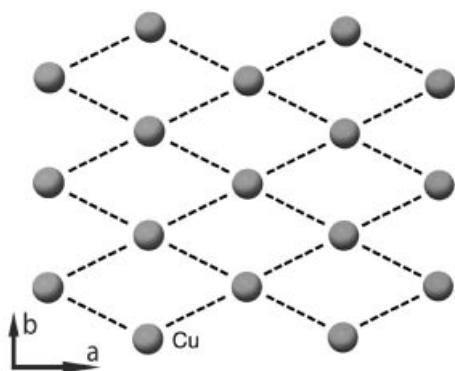


Figure 3. Drawing of the diamond-like M^{II} network in the (a,b) planes; each metal ion interacts with its four nearest neighbours as in a square planar system

cobalt(II) analogue.^[34] For the latter, it was pointed out that this racemisation, on the basis of previous studies on α -hydroxycarboxylic acids, is favoured by the use of an alkaline medium.^[36] It is worth noticing here that the present copper(II) analogue, contrary to all the other metal derivatives, can be obtained without addition of an alkaline base. Similarly, the same compound can be obtained as a powder

from the reaction under ambient rather than hydrothermal conditions. It thus appears that significant racemisation may also occur in an acidic or neutral medium, perhaps with different kinetics however.^[37]

The other M^{II} compounds were obtained as powders or very thin crystals which somewhat frustrated characterisation by single-crystal diffraction methods. However, the corresponding spectroscopic characterisations (Figure 4) and elemental analyses confirm that all complexes are isostructural with the copper(II) and cobalt(II) dimandelates described above. This was further confirmed by a comparison between their powder X-ray patterns shown in Figure 5. The powder diffraction patterns were fully indexed and the crystallographic cell parameters for the series of compounds

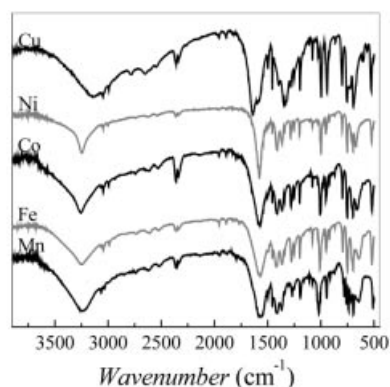


Figure 4. Infrared spectra of the transition metal mandelates; for clarity, the spectra are shifted in intensity

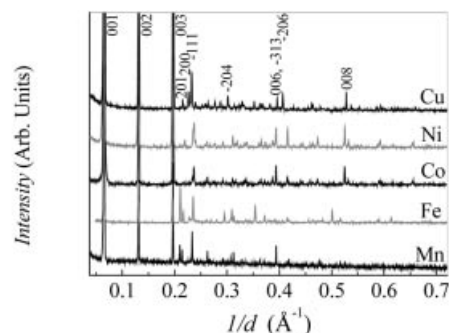


Figure 5. Comparison between the powder X-ray diffraction patterns of the five layered transition metal mandelates, shifted in intensity for clarity; some characteristic diffraction lines are labelled

Table 2. Crystallographic parameters of the first row transition metal dimandelates refined from X-ray powder patterns; all compounds crystallise in the monoclinic space group $P2_1/a$

$M(C_6H_5CH(OH)CO_2)_2$	Mn	Fe	Co	Ni	Cu ^[a]
a [Å]	8.925(5)	9.511(1)	9.3532(7)	9.239(2)	9.489(1)
b [Å]	4.933(1)	4.8370(8)	4.8737(3)	4.851(1)	4.9156(6)
c [Å]	15.605(4)	15.569(2)	15.495(1)	15.510(1)	15.551(1)
β [°]	101.31(5)	101.37(1)	99.95(1)	100.04(1)	102.749(9)
V [Å ³]	673.70(8)	702.19(6)	695.71(5)	684.49(6)	707.48(2)

^[a] Single crystal parameters are: $a = 9.454$ Å; $b = 4.905$ Å; $c = 15.495$ Å; $\beta = 102.56^\circ$; $V = 701.3$ Å³.

have been refined (Table 2) by means of a full pattern matching procedure using the Fullprof software package.^[38]

Spectroscopic Properties

The IR and UV data collected for the five compounds were easy to analyse on the basis of the crystal data (see Exp. Sect.). The IR spectra exhibit characteristic bands of the mandelate ligand. The frequency difference between the symmetric and asymmetric carboxylate vibrations, $\Delta\nu = 150\text{--}165\text{ cm}^{-1}$, is much smaller than that observed in the corresponding acid ($\Delta\nu_i \approx 270\text{ cm}^{-1}$) in agreement with the bidentate coordination mode of the carboxylate groups.^[39] The presence of broad $\nu\text{O-H}$ bands in the range $3200\text{--}3400\text{ cm}^{-1}$ is related to the mandelate OH moieties bonded to the metal ions. Interestingly, whereas the IR spectra of the Mn^{II} , Fe^{II} , Co^{II} , Ni^{II} compounds are almost identical, thus confirming very similar local structures, significant shifts of the $\nu\text{O-H}$ and carboxylate bands can be observed for Cu^{II} species. The latter is merely related to the distortion of the coordination sphere around the copper atoms due to the Jahn–Teller effect, as found from the single-crystal structure analysis (Table 1). The UV spectra are also consistent with the presence of octahedral geometries for the M^{II} ions.^[40,41] The values of Dq and the Racah parameter B have been calculated for the d^7 and d^8 ions giving $Dq = 985\text{ cm}^{-1}$, $B = 710\text{ cm}^{-1}$ and $Dq/B = 1.4$ for the Co^{II} and $Dq = 811\text{ cm}^{-1}$, $B = 977\text{ cm}^{-1}$ and $Dq/B = 0.83$ for the Ni^{II} compound in accordance with weak crystal field and high-spin configurations.^[42] For Co^{II} , admixture of forbidden d-d transitions at 480 nm (20833 cm^{-1}) and 505 nm (19801 cm^{-1}) results in a multiple structured band. A value of $Dq = 939\text{ cm}^{-1}$ can be deduced for the iron(II) ions and a shoulder at $\lambda = 1260\text{ nm}$ (7936 cm^{-1}) can be attributed to splitting of the $^5\text{E}_g$ state. The UV spectrum of the Cu^{II} derivative exhibits the usual broad band ($\lambda = 745\text{ nm}/13422\text{ cm}^{-1}$) due to transitions from the t_{2g} components to the x^2-y^2 level.

Magnetic Properties

The magnetic properties of **1**, **2**, **3**, **4** and **5** were investigated in the temperature range 2–300 K. The temperature dependence of the magnetic susceptibilities χ above 2 K is shown in Figure 6 as χT vs. T plots for **1**, **2**, **3** and **4**, after correction for diamagnetic contributions. The iron(II) compound **2** contains small amounts of an impurity which is ferromagnetic at ambient temperature. Consequently, the

susceptibility displayed in Figure 6 for this compound corresponds to the data corrected using the constant ferromagnetic moment deduced from variations in room temperature magnetisation as a function of the field.

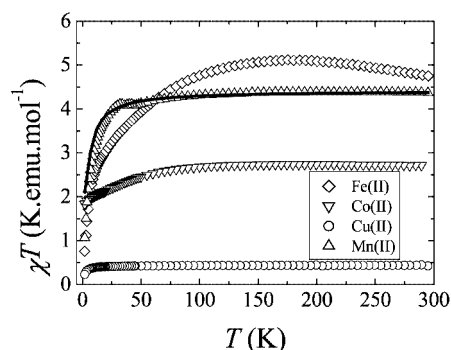


Figure 6. Temperature variation of the magnetic susceptibilities of the compounds **1**, **2**, **3** and **5** as χT vs. T plots; the full line corresponds to the fit of the data for the Mn^{II} compound **1**, as detailed in the text

The four compounds exhibit paramagnetic behaviour corresponding to quasi-isolated metal centres. The inverse-susceptibility versus T curves are linear above 200 K and were fitted using the Curie–Weiss law. The corresponding values of the Curie constants and Weiss temperatures are given in Table 3 and the corresponding values of the effective moments $\mu_{\text{eff}} = (8C)^{1/2}$ agree well with those expected for M^{II} ions in an octahedral crystal field.

Upon cooling, the χT product of the Co^{II} compound **3** exhibits a regular decrease from $2.85\text{ cm}^3\cdot\text{K}\cdot\text{mol}^{-1}$ at 300 K to $1.8\text{ cm}^3\cdot\text{K}\cdot\text{mol}^{-1}$ at 10 K. The decrease of the χT product is well understood as being due to the spin-orbit coupling effects for octahedral Co^{II} ions.^[43] Indeed, high-spin octahedral Co^{II} has a $^4\text{T}_{1g}$ ground state and, as a consequence, exhibits unquenched spin-orbit coupling in addition to a zero-field splitting which dominates at low temperature and stabilises a doublet ground state. It should be pointed out that for isolated octahedral Co^{II} ions, a minimum value of $\chi T \approx 1.8\text{ cm}^3\cdot\text{K}\cdot\text{mol}^{-1}$ can be expected corresponding to a pseudo spin $S = 1/2$ and $g \approx 4.4$. Moreover, the magnetisation vs. field variation at 2 K (not shown) is consistent with paramagnetic-like behaviour, indicating that no significant coupling takes place. The saturation moment, $M_s = 2.25\ \mu_{\text{B}}\cdot\text{mol}^{-1}$, is in agreement with the expected value for octahedral high spin Co^{II} ions ($2\text{--}3\ \mu_{\text{B}}$ per cobalt atom).^[9]

Table 3. Main magnetic data of the first row transition metal dimandelates

$\text{M}[\text{C}_6\text{H}_5\text{CH}(\text{OH})\text{CO}_2]_2$	Mn^{II}	Fe^{II}	Co^{II}	Ni^{II}	Cu^{II}
C [$\text{K}\cdot\text{emu}\cdot\text{mol}^{-1}$]	4.4	ca. 3.9	2.85	1.16	0.44
μ_{eff} [$\mu_{\text{B}}\cdot\text{mol}^{-1}$]	5.9	ca. 5.6	4.8	3.0	1.9
θ [K]	−0.8	—	−5	+11.36	−3
In-plane interactions ^[a]	AF/J = −0.122 K	isolated	isolated	F/J = +1.213 K	isolated
3D ordering ^[a]	—	—	—	F/ T_c = 2.7 K	—

^[a] AF: antiferromagnetic; F: ferromagnetic.

Although the corrected data for compound **2** are approximate owing to the presence of the magnetic impurity, the general behaviour of the susceptibility is in agreement with that expected for quasi-isolated Fe^{II} ions exhibiting spin-orbit coupling effects similar to the Co^{II} analogue above.

The copper(II) derivative show a quasi-constant χT product in the whole temperature range and is paramagnetic, whereas the Mn^{II} compound **3** exhibits a significant decrease below 30 K indicating short-range antiferromagnetic in-plane coupling. No long-range order is evident from either susceptibility or magnetisation measurements for this compound. The magnetic behaviour of **3** was modelled with the 2D Heisenberg approach in an effort to evaluate the magnitude of the nearest-neighbour exchange interaction. The susceptibility data were fit between 2 and 300 K with the high-temperature series expansion reported by Rushbrooke and Wood^[44,45,46] for an antiferromagnetic 2D Heisenberg square planar system [Equation (1)],^[47] giving $g = 2.01(1)$ and $J/k_B = -0.122(4)$ K, Figure 6. The coupling is characteristic of very weak antiferromagnetic interactions across the three-atom dicarboxylate bridge.

$$\chi_{sp}(T) = \frac{S(S+1)Ng^2\mu_B^2}{3k_B T} \times \sum_n a_n x^n \quad (1)$$

The Ni^{II} compound **4** exhibits very different behaviour. Ferromagnetic interactions are implied by the inverse susceptibility $1/\chi$ vs. T variation (not shown) with a positive Curie–Weiss temperature (Table 3). As shown in Figure 7, the temperature variation of the dc magnetic susceptibility implies the existence of a significant ferromagnetic coupling between neighbouring nickel(II) ions within the plane, with an increase in χT from 1.21 K·emu·mol⁻¹ at 295 K to 47.5 K·emu·mol⁻¹ at 2 K. Ferromagnetic long range order between the layers is demonstrated by the occurrence of a peak in the out-of-phase signal χ'' of the ac susceptibility shown in the inset of Figure 7. The Curie temperature value $T_C \approx 2.5$ K can be deduced from the maximum of χ'' where an onset of the imaginary part of the susceptibility χ'' occurs.

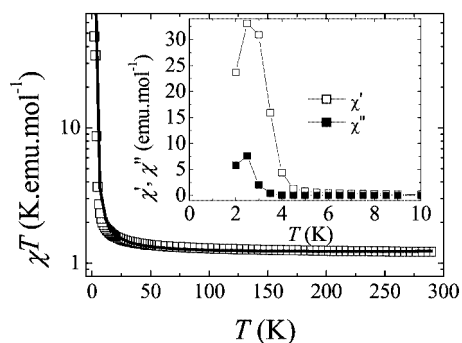


Figure 7. Temperature variation of the magnetic susceptibility of the Ni^{II} mandelate **4** as a χT vs. T plot; the full line corresponds to the fit of the data, as detailed in the text; the inset shows the variation of the real and imaginary parts of the ac susceptibility recorded in a 3.5 Oe/30 Hz magnetic field

Figure 8 shows a magnetisation loop measured at 2 K exhibiting a sharp increase in the magnetisation at low field, up to ca. the half of the saturation value. No hysteresis (at least within a few Gauss) was observed, in accordance with the isotropic character of the Heisenberg Ni^{II} ions and the magnitude of T_C . The saturation moment tends to $2\mu_B$ per Ni^{II} at 5 T which is expected at full saturation for $S = 1$ spin moments. It is important to notice, however, that M vs. H shows a smooth and quasi-linear variation in the high-field region which suggests that small canting between moments might occur, thereby explaining such particular features and leading to rather small residual moments.

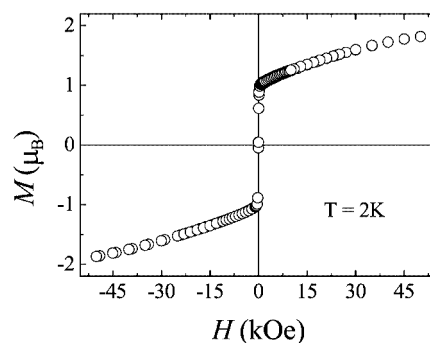


Figure 8. Magnetisation vs. field hysteresis loop for the Ni^{II} mandelate **4**, recorded at 2 K

A fit of the magnetic susceptibility above T_C was carried out using the high temperature series expansion for a ferromagnetic square planar array of $S = 1$ spins, the expression of which is similar to Equation (1) above.^[48] In this expression, the zero-field splitting (D) for Ni^{II} ions is neglected although it is known to be effective in the low temperature range, typically below 10 K.^[9] Within this approximation, the data are very well fit in the full temperature range with $g = 2.15(1)$ and $J/k_B = +1.213(4)$ K, Figure 7. Finally, the occurrence of 3D magnetic ordering can be undoubtedly established by the temperature variation of the specific heat recorded at low temperature, Figure 9. The curve shows a typical lambda anomaly, the maximum of which enables a

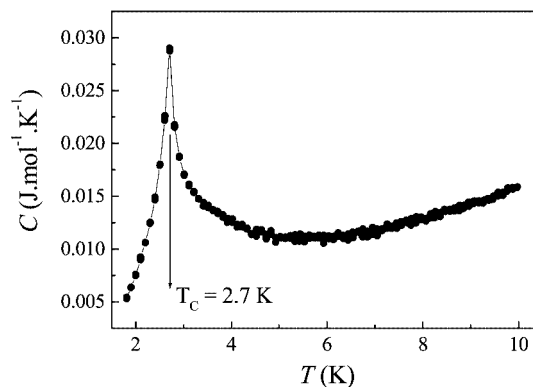


Figure 9. Low-temperature variation of the specific heat of the Ni^{II} mandelate **4**

precise determination of the Curie temperature $T_C = 2.7(1)$ K.

Conclusion

A series of Mn^{II}, Fe^{II}, Co^{II}, Ni^{II} and Cu^{II} mandelates has been crystallised and structurally and magnetically characterised. Although the starting mandelate was enantiomerically pure, the ligand was found to racemise during the synthetic process. The five compounds are isostructural with the copper analogue, the latter having been obtained as single crystals and showing a strong Jahn–Teller distortion of the coordination spheres around the Cu^{II} centres. Their solid-state structures consist of layers of six-coordinate metal(II) ions, thus forming planar arrays of octahedra interconnected through carboxylate bridges in a diamond-like network. The planes are separated by double layers of phenyl groups from the mandelate ligands resulting in a 2D system. From a magnetic point of view, it has been shown that the in-plane exchange pathways between neighbouring magnetic centres form a square-like planar array. The exchange coupling involving bridging carboxylate ligands in a *syn-anti* conformation is known to promote antiferromagnetic interactions between neighbouring M^{II} ions^[49] and to be more favourable than the *anti-anti* conformation.^[24] This agrees with the observed behaviour of the χT product for the series of transition metal mandelates except for the nickel derivative for which ferromagnetic behaviour is observed with ferromagnetic 3D ordering at $T_C = 2.7$ K.

Experimental Section

General Remarks: Thermogravimetric experiments were performed using a Setaram TG92 instrument (heating rate of 3 °C/min, air stream). FT-IR studies were performed with an ATI Mattson Genesis computer-driven instrument (0.1 mm thick powder samples in KBr). UV/Vis/NIR studies were performed with a Perkin–Elmer Lambda 19 instrument (spectra recorded by reflection with a resolution of 4 nm and a sampling rate of 480 nm/min). Elemental analyses were performed using a Thermo-Finnigan EA 1112 setup (Service d'analyses, ICS, Strasbourg, France). Magnetic studies were carried out using a Quantum Design SQUID MPMS-XL magnetometer (± 5 T, 2–300 K) on several sets of crystalline or powdered samples. Low temperature specific heat measurements were carried out using a MagLab HC Oxford Instrument. Powder X-ray diffraction patterns for the whole series were obtained using Bragg–Brentano Siemens D500 (Co- $K_{\alpha 1}$, $\lambda = 1.78897$ Å) and D5000 (Cu- $K_{\alpha 1}$, $\lambda = 1.5406$ Å) diffractometers equipped with primary beam monochromators. All the powder X-ray patterns exhibit large preferential orientations of the crystallites parallel to the stacking axis c .

X-ray Crystallographic Study: A single crystal of the copper mandelate **5** was mounted on a Nonius Kappa-CCD area detector diffractometer (Mo- K_{α} , $\lambda = 0.71073$ Å). The complete conditions of data collection (Denzo software) and structure refinements are given below. The cell parameters were determined from reflections taken from one set of 10 frames (1.0° steps in ϕ angle), each with an exposure time of 20 s. The structure was solved by direct methods

(SHELXS-97) and refined against F^2 using the SHELXL-97 software.^[50] The absorption was corrected empirically with Sor-tav.^[51] All non-hydrogen atoms were refined anisotropically. Hydrogen atoms were generated according to stereochemistry and refined using a riding model in SHELXL-97. CCDC-236368 contains the supplementary crystallographic data for this paper. These data can be obtained free of charge at www.ccdc.cam.ac.uk/conts/retrieving.html [or from the Cambridge Crystallographic Data Centre, 12 Union Road, Cambridge CB2 1EZ, UK; Fax: (internat.) + 44-1223-336-033; E-mail: deposit@ccdc.cam.ac.uk]. Green-blue crystal, crystal dimension: 0.13 × 0.10 × 0.02 mm, C₁₆H₁₄CuO₆, $M = 365.81$ g·mol⁻¹, monoclinic space group $P2_1/a$, $a = 9.454(5)$ Å, $b = 4.905(5)$ Å, $c = 15.495(5)$ Å, $\beta = 102.564(5)^\circ$, $Z = 2$, $D_{\text{calcd.}} = 1.732$ g·cm⁻³, μ (Mo- K_{α}) = 1.588 mm⁻¹, $T_{\text{min.}} = 0.890$, $T_{\text{max.}} = 0.970$ mm, a total of 2406 reflections, $2.69^\circ < \theta < 31.96^\circ$, 2406 independent reflections with 1833 having $I > 2\sigma(I)$, 106 parameters, Final results: $R_1 = 0.0817$, $wR_2 = 0.1349$, $Gof = 1.16$, maximum residual electronic density = 1.152 e⁻Å⁻³.

Manganese(II) Dimandelate, C₁₆H₁₄O₆Mn (1): C₁₆H₁₄O₆Mn (1) was synthesised by a hydrothermal method from MnCl₂·4H₂O (99% Aldrich), (*R*)-mandelic acid (98% Acros) and NaOH (Merck). The starting mixture, which consisted of [MnCl₂·4H₂O], C₈H₈O₃, NaOH and H₂O in a ratio of 2:4:4:20, was homogenised and transferred to a sealed Teflon lined hydrothermal bomb (120-mL bomb volume). After heating at 170 °C for 120 h under autogenous pressure, a white, slightly pink crystalline powder was obtained which was washed and rinsed with distilled water and absolute ethyl alcohol (yield: 0.43 g, 60% on the basis of MnCl₂·6H₂O). The purity was confirmed by elemental analysis [C₁₆H₁₄O₆Mn (361.21): calcd. C 53.80, H 3.95; found C 53.21, H 3.85] and oxidising pyrolysis [heating in air from 20 to 700 °C at 3 °C/min, at 700 °C for 30 min to transform manganese into Mn₂O₃ and cooling to 20 °C at 10 °C/min: calcd. Mn 15.38%; found 17.16%]. IR (KBr pellet): $\tilde{\nu} = 3237$ cm⁻¹ (νOH), 1560 cm⁻¹ (ν_{asym}CO) and 1413 cm⁻¹ (ν_{sym}CO).

Iron(II) Dimandelate C₁₆H₁₄O₆Fe (2): C₁₆H₁₄O₆Fe (2) was synthesised by a hydrothermal method according to the same process as for the manganese analogue **1** but using FeCl₂·6H₂O instead of Mn^{II} dichloride. A very pale green crystalline powder was obtained, washed and rinsed with distilled water and absolute ethyl alcohol (yield: 0.36 g, 50% on the basis of FeCl₂·6H₂O). The purity was checked by elemental analysis [C₁₆H₁₄O₆Fe (358.12): calcd. C 53.66, H 3.94; found C 53.63, H 3.91] and oxidising pyrolysis [heating in air from 20 to 700 °C at 2 °C/min, at 700 °C for 30 min to transform into Fe₃O₄ and cooling to 20 °C at 10 °C/min: calcd. Fe 15.59%; found 18.85%]. IR (KBr pellet): $\tilde{\nu} = 3247$ cm⁻¹ (νOH), 1565 cm⁻¹ (ν_{asym}CO) and 1417 cm⁻¹ (ν_{sym}CO). UV/Vis (reflectance for octahedral coordination of Fe^{II}): $\lambda = 1065$ nm (⁵E_g → ⁵T_{2g}).

Cobalt(II) Dimandelate C₁₆H₁₄O₆Co (3): C₁₆H₁₄O₆Co (3) was synthesised similarly to the above procedure but starting from CoCl₂·6H₂O (98% Acros). Very thin pink platelet-like crystals were obtained, washed and rinsed with distilled water and absolute ethyl alcohol (yield: 0.47 g, 65% on the basis of CoCl₂·6H₂O). The purity was confirmed by elemental analysis [C₁₆H₁₄CoO₆ (361.21): calcd. C 53.20, H 3.91; found C 52.84, H 3.85] and oxidising pyrolysis [heating in air from 20 to 700 °C at 3 °C/min, at 700 °C for 30 min to transform into Co₃O₄ and cooling to 20 °C at 10 °C/min: calcd. Co 16.32%; found 16.78%]. IR (KBr pellet): $\tilde{\nu} = 3255$ cm⁻¹ (νOH), 1573 cm⁻¹ (ν_{asym}CO) and 1408 cm⁻¹ (ν_{sym}CO). UV/Vis (reflectance for octahedral coordination of Co^{II}): $\lambda = 1140$ nm (⁴T_{1g} → ⁴T_{2g}), 645 nm (⁴T_{1g} → ⁴A_{2g}), 545 nm [⁴T_{1g} → ⁴T_{1g} (P)].

Nickel(II) Dimandelate $C_{16}H_{14}O_6Ni$ (4): $C_{16}H_{14}O_6Ni$ (4) was synthesised in the same manner as above from $NiCl_2 \cdot 6H_2O$ (99.99% Sigma). A green powder was obtained, washed and rinsed with distilled water and absolute ethyl alcohol (yield: 0.5 g, 70% on the basis of $NiCl_2 \cdot 6H_2O$). The purity was confirmed by elemental analysis [$C_{16}H_{14}NiO_6$ (360.97): calcd. C 53.24, H 3.91; found C 53.15, H 3.87] and oxidising pyrolysis [heating in air from 20 to 700 °C at 3 °C/min, at 700 °C for 30 min to transform into NiO, and cooling to 20 °C at 10 °C/min: calcd. Ni 16.26%; found 17.48%]. IR (KBr pellet): $\tilde{\nu} = 3245\text{ cm}^{-1}$ (vOH), 1577 cm^{-1} ($\nu_{\text{asym}}\text{CO}$) and 1411 cm^{-1} ($\nu_{\text{sym}}\text{CO}$). UV/Vis (reflectance for octahedral coordination of Ni^{II}): $\lambda = 410\text{ nm}$ (${}^3A_{2g} \rightarrow {}^3T_{2g}$), 685 nm (${}^3A_{2g} \rightarrow {}^3T_{1g}$), 745 nm (${}^3A_{2g} \rightarrow {}^1E_g$), 1235 nm [${}^3A_{2g} \rightarrow {}^3T_{1g}(P)$].

Copper(II) Dimandelate $C_{16}H_{14}O_6Cu$ (5): $C_{16}H_{14}O_6Cu$ (5) was synthesised from $CuCl_2 \cdot 2H_2O$ (99% Aldrich) and (*R*)-mandelic acid (98% Acros). The starting mixture, corresponding to $CuCl_2 \cdot 2H_2O$, $C_8H_8O_3$ and H_2O in a molar ratio of 2:4:20, was homogenised and transferred to a sealed, Teflon-lined hydrothermal bomb (120-mL bomb volume). Hydrothermal treatment (170 °C, 72 h, autogenous pressure) led to white-yellow crystals and a blue-green solution. These crystals were left to dissolve in the mother liquor. After 6 d, large green-blue crystals of 5 suitable for single-crystal X-ray diffraction analysis were obtained. The crystals were washed with distilled water and absolute ethyl alcohol. (yield: 0.38 g, 52% on the basis of $CuCl_2 \cdot 2H_2O$). The purity was confirmed by elemental analysis [$C_{16}H_{14}O_6Cu$ (365.82): calcd. C 53.66, H 3.94; found C 53.63, H 3.91] and oxidising pyrolysis [heating in air from 20 to 700 °C at 3 °C/min, at 700 °C for 30 min to transform into CuO and cooling to 20 °C at 10 °C/min: calcd. Cu 17.37%; found 16.99%]. IR (KBr pellet): $\tilde{\nu} = 3133\text{ cm}^{-1}$ (vOH), 1635 cm^{-1} ($\nu_{\text{asym}}\text{CO}$) and 1456 cm^{-1} ($\nu_{\text{sym}}\text{CO}$). UV/Vis (reflectance for octahedral coordination of Cu^{II}): $\lambda = 745\text{ nm}$ (transition from t_{2g} components to $x^2 - y^2$).

- [1] *Research Frontiers in Magnetochemistry* (Ed.: C. O'Connor), World Scientific Publishers, Singapore, 1993.
- [2] *Magnetic Molecular Materials* (Eds.: D. Gatteschi, O. Kahn, J. S. Miller, F. Palacio), Kluwer, Dordrecht, 1991.
- [3] L. P. Kadanoff, W. Götzke, D. Hamblen, R. Hecht, E. A. S. Lewis, V. V. Palciauskas, M. Rayl, J. Swift, *Rev. Mod. Phys.* **1967**, 39, 395–431.
- [4] L. J. de Jongh, A. R. Miedema, *Adv. Phys.* **1974**, 23, 1–260.
- [5] See for instance the articles in *Magnetism: Molecules to Materials-Models and Experiments* (Eds.: J. S. Miller, M. Drillon), Wiley-VCH, Weinheim, 2001.
- [6] J.-P. Renard, in *Organic and inorganic Low-dimensional crystal-line materials* (Eds.: P. Delhaes, M. Drillon), NATO-ASI Series, Plenum Press New York and London, 1987, p. 125–140.
- [7] C. Janiak, *Dalton Trans.* **2003**, 2781.
- [8] S. L. James, *Chem. Soc. Rev.* **2003**, 32, 276.
- [9] R. L. Carlin, *Magnetochemistry*, Springer-Verlag, Berlin, Heidelberg, 1986; O. Kahn, *Molecular Magnetism*, Wiley-VCH, Weinheim, 1993.
- [10] Book review: *Molecular Magnets – Recent Highlights* (Eds.: W. Linert, M. Verdaguer), Springer, Wien, New York, 2003.
- [11] *Molecular Magnetism* (Eds.: K. Itoh, M. Kinoshita), Kodansha Ltd. and Gordon and Breach Science Publishers, Amsterdam, London, 2000.
- [12] M. Drillon, P. Panissod, *J. Magn. Magn. Mater.* **1998**, 188, 93–99.
- [13] *Magnetic Properties of Layered Transition Metal Compounds* (Ed.: L. J. de Jongh), vol. 9A (“Physics and Chemistry of Materials with Low-dimensional Structures”), Kluwer Academic Publishers, Dordrecht, 1990.
- [14] P. Rabu, S. Rouba, V. Laget, C. Hornick, M. Drillon, *Chem.*

- Commun.* **1996**, 10, 1107–1108; W. Fujita, K. Awaga, *Inorg. Chem.* **1996**, 35, 1915–1917; P. Rabu, J. M. Rueff, Z. L. Huang, S. Angelov, J. Souletie, M. Drillon, *Polyhedron* **2001**, 20, 1677–1685; P. Rabu, M. Drillon, K. Awaga, W. Fujita, T. Sekine, in *Magnetism: Molecules to Materials* (Eds.: J. S. Miller, M. Drillon), Wiley-VCH, Weinheim, Germany, 2001, p. 357–395.
- [15] P. Rabu, P. Janvier, B. Bujoli, *J. Mater. Chem.* **1999**, 9, 1323–1326.
- [16] Z.-L. Huang, M. Drillon, N. Masciocchi, A. Sironi, J.-T. Zhao, P. Rabu, P. Panissod, *Chem. Mater.* **2000**, 12, 2805–2812.
- [17] S. O. H. Gutschke, D. J. Price, A. K. Powell, P. T. Wood, *Angew. Chem. Int. Ed.* **2001**, 40, 1920–1923.
- [18] D. J. Price, S. Tripp, A. K. Powell, P. T. Wood, *Chem. Eur. J.* **2001**, 7, 200–208.
- [19] R. Feyerherm, A. Loose, P. Rabu, M. Drillon, *Solid State Science* **2003**, 5, 321–326.
- [20] Y. Rodriguez-Martin, C. Ruiz-Perez, J. Sanchiz, F. Lloret, M. Julve, *Inorg. Chim. Acta* **2001**, 318, 159165; C. Ruiz-Pérez, J. Sanchiz, M. Hernández-Molina, F. Lloret, M. Julve, *Inorg. Chim. Acta* **2000**, 298, 202–208.
- [21] M. Riou-Cavellec, C. Albinet, C. Livage, N. Guillou, M. Nogués, J. M. Grenèche, G. Férey, *Solid State Sciences* **2002**, 4, 267–270.
- [22] M. J. Plater, M. R. S. J. Foremen, R. A. Howie, J. M. S. Skakle, A. M. Z. Slawin, *Inorg. Chim. Acta* **2001**, 315, 126–132.
- [23] N. Snejko, E. Guttierrez-Puebla, J. L. G. Smith, D. E. Lynch, T. C. W. Mak, W.-H. Yip, C. H. L. Kennard, M. A. Monge, C. Ruiz-Valero, *Chem. Mater.* **2002**, 14, 1879–1883.
- [24] J. M. Rueff, N. Masciocchi, P. Rabu, A. Sironi, A. Skoulios, *Chem. Eur. J.* **2002**, 2813–2820; J. M. Rueff, N. Masciocchi, P. Rabu, A. Sironi, A. Skoulios, *Eur. J. Inorg. Chem.* **2001**, 2843–2848.
- [25] G. Smith, D. E. Lynch, T. C. W. Mak, W.-H. Yip, C. H. L. Kennard, *Polyhedron* **1993**, 12, 203–208.
- [26] G. Smith, O. J. O'Reilly, C. H. L. Kennard, *J. Chem. Soc., Dalton Trans.* **1980**, 2462–2466.
- [27] T. Asaji, K. Aoki, D. Nakamura, *Z. Naturforsch., Teil A* **1984**, 39, 371–375.
- [28] R. Carballo, A. Castinieras, S. Balboa, B. Covelo, J. Niclos, *Polyhedron* **2002**, 21, 2811.
- [29] R. Carballo, B. Covelo, S. Balboa, A. Castinieras, J. Niclos, *Z. Anorg. Allg. Chem.* **2001**, 627, 948.
- [30] D. A. House, J. Browning, J. R. Ripal, W. T. Robinson, *Inorg. Chim. Acta* **1999**, 292, 73.
- [31] I. K. Smatanova, J. Marek, P. Svancarek, P. Schwendt, *Acta Crystallogr., Sect. C* **2000**, 56, 154.
- [32] G. Meister, G. Rheinwald, H. Stoeckli-Evans, G. Suss-Fink, *J. Organomet. Chem.* **1995**, 496, 197.
- [33] [33a] K. N. Kovalenko, D. V. Kazachenko, V. P. Kurbatov, L. G. Kovaleva, *Zh. Neorg. Khim.* **1971**, 16, 2444. [33b] A. Ranade, *Z. Anorg. Allg. Chem.* **1972**, 388, 105. [33c] P. V. Khadikar, R. L. America, *Ind. J. Chem.* **1975**, 13, 525. [33d] A. B. Sen, S. N. Kapoor, *J. Prakt. Chem.* **1963**, 20, 237. [33e] R. Larsson, B. Folkesson, *Acta Chem. Scand.* **1968**, 22, 1970–1980. [33f] A. J. Fischinger, A. Sarapu, A. Companion, *Can. J. Chem.* **1969**, 47, 2629–2637. [33g] P. Spacu, S. Plostinaru, L. Patron, A. Contescuand, N. Stanica, *Rev. Roum. Chim.* **1985**, 30, 837–842. [33h] R. P. Rajguru, C. Panda, *J. Inst. Chem. (India)* **1991**, 63, 37–39.
- [34] H. Kumagai, Y. Oka, K. Inoue, M. Kurmoo, *J. Phys. Chem. Sol.* **2004**, 65, 55–60.
- [35] C. Janiak, *J. Chem. Soc., Dalton Trans.* **2000**, 3885–3896.
- [36] I. L. Finar, *Organic Chemistry*, 4th ed., Longmans, London, 1968, vol. 2, p. 69.
- [37] Winther, *Z. Physik Chem.* **1906**, 56, 465–511; A. N. Campbell, A. J. R. Campbell *J. Am. Chem. Soc.* **1932**, 54, 3834–3841; A. N. Campbell, A. J. R. Campbell *Nature* **1932**, 129, 281.
- [38] Fullprof: J. Rodriguez-Carvajal, *Physica* **1993**, B192, 55.
- [39] K. Nakamoto, *Infrared and Raman Spectra of Organic and Co-*

- ordination Compounds*, 4th ed., Wiley – Interscience Publication, New York, **1986**, 231.
- [40] A. B. P. Lever, *Inorganic Electronic Spectroscopy*, 2nd ed., Elsevier, Amsterdam, **1984**.
- [41] L. Banci, A. Bencini, C. Benelli, D. Gatteschi, C. Zanchini, *Struct. Bonding* **1982**, 52, 37–86.
- [42] Y.-S. Dou, *J. Chem. Educ.* **1990**, 67, 134.
- [43] F. E. Mabbs, D. J. Machin, *Magnetism and transition metal complexes*, Chapman and Hall Ltd., London, **1973**.
- [44] G. S. Rushbrooke, G. A. Baker, P. J. Wood, in *Phase Transitions and Critical Phenomena* (Eds.: C. Domb, M. S. Green), Academic Press, London, New York, **1974**, vol. III, chapter 5.
- [45] K. Yamaji, J. J. Kondo, *Phys. Soc. Jpn.* **1973**, 35, 25–32.
- [46] R. Navarro, in *Magnetic Properties of Layered Transition Metal Compounds* (Ed.: L. J. de Jongh), Kluwer Academic Publishers, Dordrecht, Boston, London, **1990**, p. 105–190.
- [47] $x = -J/(k_B T)$ for antiferromagnetic coupling, N = Avogadro's number, μ_B = Bohr magneton, g = Lande g value, $a_1 = 23.33333$, $a_2 = 396.66666$, $a_3 = 6212.888888$, $a_4 = 87638.8119558377$, $a_5 = 1161923.54664125$, $a_6 = 14796191.6938613$, $a_7 = 180849416.031247$, and $a_8 = 2142650986.87194$.
- [48] $x = J/(k_B T)$ for ferromagnetic coupling, $a_1 = 5.333333333$, $a_2 = 18.66666667$, $a_3 = 56.88888889$, $a_4 = 152.3950631$, $a_5 = 376.9415553$, $a_6 = 918.8538407$, $a_7 = 2134.805724$, and $a_8 = 4572.414518$.
- [49] E. Coronado, M. Drillon, D. Beltran, J. C. Bernier, *Inorg. Chem.* **1984**, 23, 4000–4004.
- [50] G. M. Sheldrick, *SHELXL-97*, University of Göttingen, Germany, **1997**.
- [51] Sortav: R. H. Blessing, *J. Appl. Crystallogr.* **1989**, 22, 396–397.

Received July 17, 2004
Published Online January 3, 2005